

Histological and histochemical changes in the peripheral organs of the immune system of dogs in cases of isoniazid poisoning

G. I. Kotsyumbas, N. P. Vretsona

Stepan Gzhytskyi National University of Veterinary Medicine and Biotechnology, Lviv, Ukraine

Article info

Received 29.06.2021

Received in revised form
01.08.2021

Accepted 02.08.2021

Stepan Gzhytskyi National
University of Veterinary
Medicine and Biotechnology,
Pekarska st., 50,
Lviv, 79010, Ukraine.
Tel.: +38-093-749-45-68.
E-mail:
nataliya.vretsona@gmail.com

Kotsyumbas, G. I., & Vretsona, N. P. (2021). Histological and histochemical changes in the peripheral organs of the immune system of dogs in cases of isoniazid poisoning. *Regulatory Mechanisms in Biosystems*, 12(3), 537–544. doi:10.15421/022174

Most publications on isoniazid poisoning in dogs are devoted to clinical diagnostics, treatment, and prevention of the disease. Histological and histochemical changes are not fully described, though they are important in assessing the toxic effects of isoniazid. Isoniazid is used to treat tuberculosis in humans. Dogs are hypersensitive to this drug. The article highlights the results of macroscopic, histological, and histochemical studies of the dogs' lymph nodes and spleen in cases of isoniazid poisoning. A pathological examination of 19 corpses of dogs of different ages was performed, during which isoniazid poisoning was posthumously diagnosed, based on anamnesis, clinical signs, pathological autopsy, histological, and histochemical examination. Samples of lymph nodes and spleen were fixed in a 10% aqueous neutral formalin solution, Carnoy's solution, and Bouin's fixative. Histocuts were prepared using a sled microtome and stained with hematoxylin and eosin. Staining was also performed according to the techniques suggested by McManus, Brachet, and Perls. The pathomorphological changes in lymph nodes and spleen were characterized by disorganization of vascular walls and connective tissue fibers of the stroma, dilatation of veins, their overflow with hemolyzed blood, and, in cases of the long clinical course, thrombosis of small vessels. Intravascular hemolysis of erythrocytes resulted in an excessive formation of hemosiderin. Histochemically, the spleen and lymph nodes showed a significant increase in the number of hemosiderophages in the spleen's red and white pulp and the lymph nodes' central sinuses and pulp cords. In the spleen, mucoid swelling and necrobiotic changes in the wall structures of the arterioles and arteries progressed with a narrowing of their lumen in dogs suffering from the long clinical course. Increased permeability of the microcirculatory tract vessels of the spleen and lymph nodes, transudate formation, and the destructive changes in the reticular skeleton accompanied hemodynamic violations. A sharp change in blood rheology caused the violation of trophism and metabolism in the immune system. Lymphoid elements of the lymph nodes and white pulp of the spleen were in a state of karyorrhexis and karyolysis. The morphological study of the immune system's peripheral organs suggests that dogs poisoned by isoniazid demonstrate hemodynamic disorders, changes in the physicochemical properties of blood (hemolysis of erythrocytes and thrombosis). This is the basis of trophic disorders, metabolic malfunctions, and the development of dystrophic processes in all structural elements of the spleen and lymph nodes.

Keywords: pathological examinations; lymph nodes; spleen; dystrophic changes; hemodynamic violations; necrobiotic changes.

Introduction

Isoniazid poisoning of dogs has recently become increasingly common in various regions of Ukraine. Isoniazid, i.e., an isonicotinic acid hydrazide, is widely available as an anti-tuberculosis drug and used in human medicine for therapeutic purposes (Lee et al., 2019). The drug absorbs well in the gastrointestinal tract (within 30 minutes). It is metabolized by the liver by means of the cytochrome P-450 system. The time necessary to reach the maximum concentration in the blood (T_{max}) is 1–4 hours. The high sensitivity of dogs to isoniazid results from the low activity of N-acetyltransferase in their liver. The LD_{50} of isoniazid for dogs amounts to 50 mg/kg. Isoniazid derivatives easily bind to pyridoxine, which leads to blocking of its absorption by the organism. This results in a sharp decrease in the synthesis of gamma-aminobutyric acid and is functionally expressed by the development of seizures, hypoglycemic coma, and, finally, death (Chin et al., 1978, 1981).

When isoniazid enters the animal's organism, it spreads through the bloodstream and causes irreversible changes. Isoniazid easily penetrates the blood-brain barrier and can be found in various tissues and body fluids. In addition, isoniazid hydroxylates forming hydrazones with pyruvic and α -ketoglutaric acid (Chuvina et al., 2018).

After poisoning, the concentration of isoniazid in the dog's organism reaches its maximum in two hours. The first signs of drug poisoning appear in 30–60 minutes. Typical signs include drowsiness, loss of coordina-

tion (ataxia), tremors and weakness in the extremities, hypersalivation, vomiting (often bloody), convulsions, followed by respiratory and cardiac depression, and coma. In the absence of treatment, death occurs within 3 hours in almost 100% of cases (Villar et al., 1995). The principle of the drug's toxic action is based on the inability of the dog's organism to metabolize isoniazid effectively (due to the low activity of N-acetyltransferase) (Sarich et al., 1999). The formation of isoniazid-pyridoxine complexes leads to pyridoxine deficiency and, as a consequence, a decrease in the synthesis of gamma-aminobutyric acid. This acid is involved in the inhibition processes in the central nervous system, and also has an antihypoxic effect. Decreased gamma-aminobutyric acid synthesis leads to hypoxia, seizures, asphyxia, hypoglycemic coma, and finally, to the animal's death.

Many authors recorded the following macroscopic changes during the autopsy of dogs who died from isoniazid poisoning: general venous hyperemia, acute dilatation of the right half of the heart, acute congestive hyperemia and pulmonary edema, acute catarrhal gastroenteritis, acute congestive hyperemia and dystrophy of the liver and kidneys, and pancreatic necrosis (Boelsterli & Lee, 2014; Schmid et al., 2017).

According to the references, isoniazid persists very long in corpses stored in the open air. In the stomach, small intestine, and kidneys, isoniazid and its breakdown products are stored for 5 months, in the liver – 4 months, in the brain – 3 months. When burying corpses in the ground, the duration of tubazide storage is reduced: in the stomach, small intestine, and kidneys it is up to 4 months, in the liver and brain – up to 3 months.

Analyzing the scientific references, it should be noted that a significant amount of scientific work is devoted to the study of the drug's pharmacological properties. However, structural and functional changes in the organs and tissues under the influence of isoniazid are covered insufficiently (Villar et al., 1995; Kucenko, 2004; Kucenko et al., 2004). Therefore, our work aims to study the morphological peculiarities of changes in the lymph nodes and spleen of dogs that died of isoniazid poisoning.

Materials and methods

All the manipulations with the animals were conducted according to the European Convention for the Protection of Vertebrate Animals used for Experimental and other Scientific Purposes (Official Journal of the European Union L276/33, 2010).

The research was based on macroscopic, histological, and histochemical study of the lymph nodes and spleen, selected from 19 carcasses of dogs that died of isoniazid poisoning. Pathological autopsy of dogs of different ages and breeds was performed, namely: Cocker Spaniel (5 years old), Labrador (7 years old), German Shepherd (1-year-old), Beagle (2 years old), Yorkshire Terrier (4 years old), German Shepherd (8 years old), half-breed dog (5 years old), Pekingese (3 years old), German Shepherd (3 years old), Labrador (4 years old), German Shepherd (1.5 years old), Dachshund (2 years old), Husky (4 years old), Cocker Spaniel (2 years old), outbred dog (6 years old), German Shepherd (7 years old), outbred dog (3 years old).

A pathological autopsy of dog carcasses was performed according to the Shor method, with complete evisceration of the internal organs. During the autopsy, samples were taken from the peripheral organs of the immune system of dogs (lymph nodes and spleen). The samples were fixed in 10% aqueous solution of neutral formalin, Carnoy's fixative, and Bouin's fluid. Dehydration was performed in ethanol of increasing concentration; the samples were compacted and poured into paraffin. Histocuts with a thickness of 7 μm were prepared on MC-2 microtome and stained with hematoxylin and eosin according to the techniques suggested by Perls, Brachet, and McManus. Histological and histochemical changes of histopreparations were studied with Leica DM-2500 microscope (Switzerland). Photo fixation was performed with a Leica DFC 450-C camera and Leica Application Suite Version 4.4.

Results

During the pathological autopsy of dog carcasses, macroscopic changes in the spleen differed slightly, depending on the dose and physiological state of the animal. These factors determined a different duration of the clinical course. The spleen was mostly flattened, irregularly boot-shaped with a widened lower end. In animals that died within 3–4 hours after isoniazid poisoning, the spleen was filled with blood, the edges were rounded and of a brown-cherry colour (Fig. 1a). The spleen of animals that died after four hours became sluggish, greyish-brown, and frequently with dark-blue cells. The capsule of the spleen was wrinkled (Fig. 1b).



Fig. 1. Spleen of a dog poisoned with isoniazid (macroscopic changes):

a – a dog that died four hours after the onset of poisoning symptoms; *b* – dog that died six hours after the onset of poisoning symptoms

Histological examination of the spleen revealed a sharp violation of hemodynamics, destruction of the walls of veins, arteries, and connective tissue skeleton, severe disorganization of elastic fibers, and fragmentation of the red pulp's reticular skeleton. At the same time, the hemolyzed blood of a homogeneous light violet shade prevailed in sharply expanded gleams of venous sinuses. Blood filling of capillaries with dilatation of small veins indicated the increased inflow of blood through the system of arteries (Fig. 2a). The contours of the venules and veins' walls were visible due to their permeation with blood plasma and the basement membranes' fuchsinophilia (Fig. 2b).

The structural organization of smooth muscles, trabecular and pulp cords' collagen fibers, and central arteries underwent significant changes. The connective tissue fibers and smooth muscle fibers of the trabeculae were fluffy and impregnated with transudate (Fig. 2c). The adventitia lost its fibrousness and turned into a pale pink homogeneous mass in the trabecular arteries. The structure of smooth muscles, elastic, and collagen fibers in the walls of the arteries was disorganized. The elastic membrane of the intima was fluffy. The dilated lumens between the smooth muscle fibers made the walls of the arterioles look porous. The progression of necrobiotic processes in the walls of blood vessels was also indicated by the changes in the nuclei, which were lysed in most fibers. Also, lysed blood cells predominated in the lumen of the arteries (Fig. 2d). Intense destruc-

tion of smooth muscle, elastic, and collagen fibers in the walls of blood vessels and trabeculae caused hemodynamic disturbances and blood deposition in the venous sinuses.

On the preparations with Brachet staining, white pulp's lymph nodes were small in size, with no delineated areas, and were mainly represented by the periarterial area (Fig. 2e). The lymph nodes' central arteries were also altered, i.e., the basement membrane was thickened, folded, fragmented, and impregnated with PAS-positive compounds. The endothelium was swollen and desquamated endothelial cells were detected in the lumen (Fig. 4a). The revealed changes in the vessel walls indicated a sharp inhibition of trophism and metabolism in cells. Most cells of lymphoid nodules were in a state of karyorrhexis, which indicated the progression of necrobiotic processes in the lymphoid elements (Fig. 2f). On the preparations with Perls staining, blue inclusions visualized in the macrophage elements among the fluffy T-lymphocytes of the lymph nodes (Fig. 2g).

It is known that the macrophage of red pulp elements carry out phagocytosis not only of the corpuscular elements that flow with the blood, but also of hemosiderin, which is released after the breakdown of erythrocytes. In addition, the spleen experiences a large functional load in terms of the increased hemolysis of erythrocytes. In such case, the reticular cells of the spleen most frequently become siderophages. Hemosiderin freely enters the intercellular substance after the disintegration of siderophages.

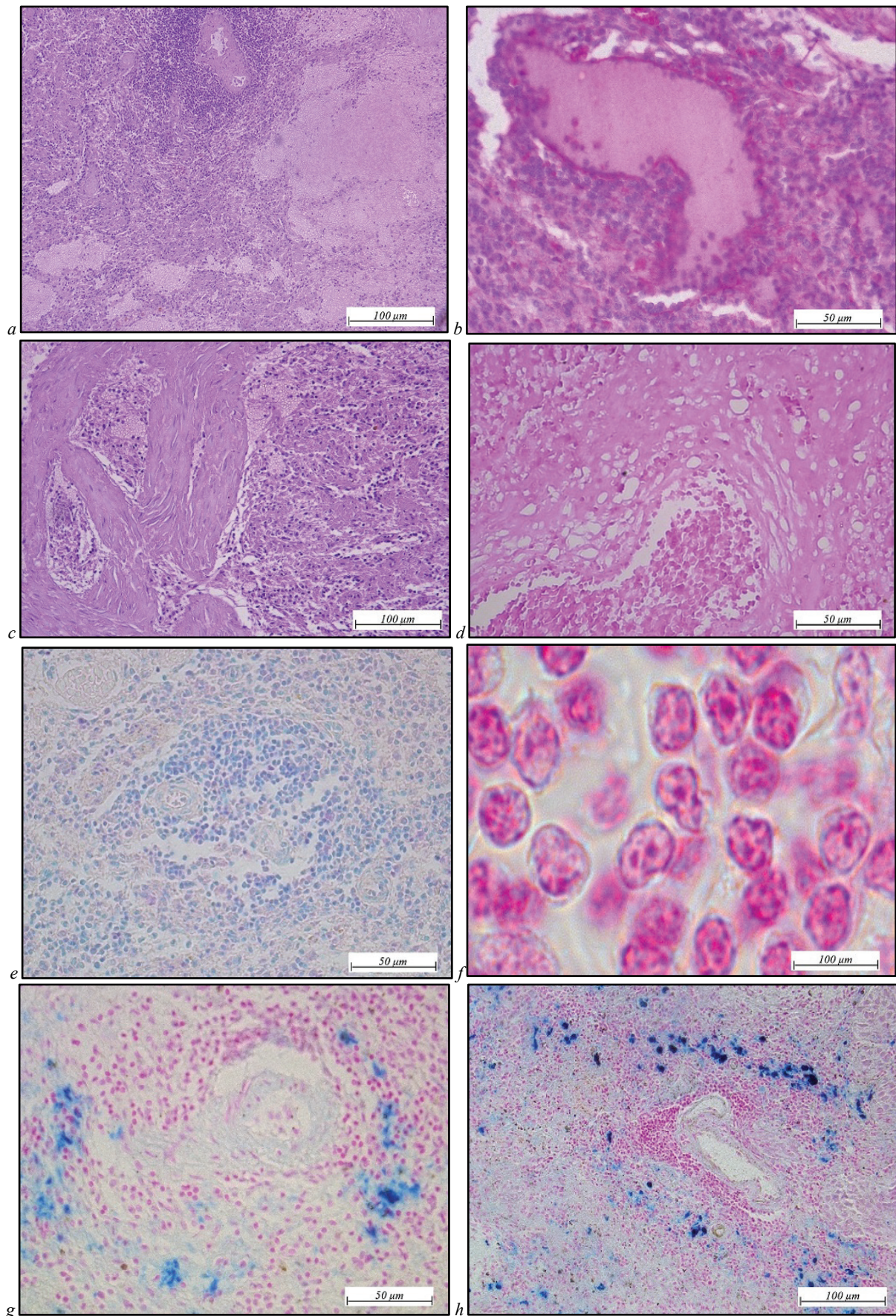


Fig. 2. The spleen of a dog poisoned with isoniazid (histological examination): *a* – the red pulp is filled with hemolyzed blood, McManus; *b* – Vein dilatation; fuchsinophilic wall of the venule; the lumen of the vein is filled with plasma, McManus; *c* – trabeculae; connective tissue fibers of the trabeculae are fluffy and impregnated with transudate, McManus; *d* – trabecular artery of the spleen; smooth muscle fibers are retouched; nuclei are lysed, hematoxylin and eosin; *e* – the periarterial zone of the lymph node is loose and filled with T-lymphocytes, Brachet; *f* – T-lymphocytes in the state of karyorrhexis, Perls; *g* – hemosiderophages in the lymph node, perls; *h* – spleen of a dog that died three hours after the poisoning; siderophages in the red pulp, Perls

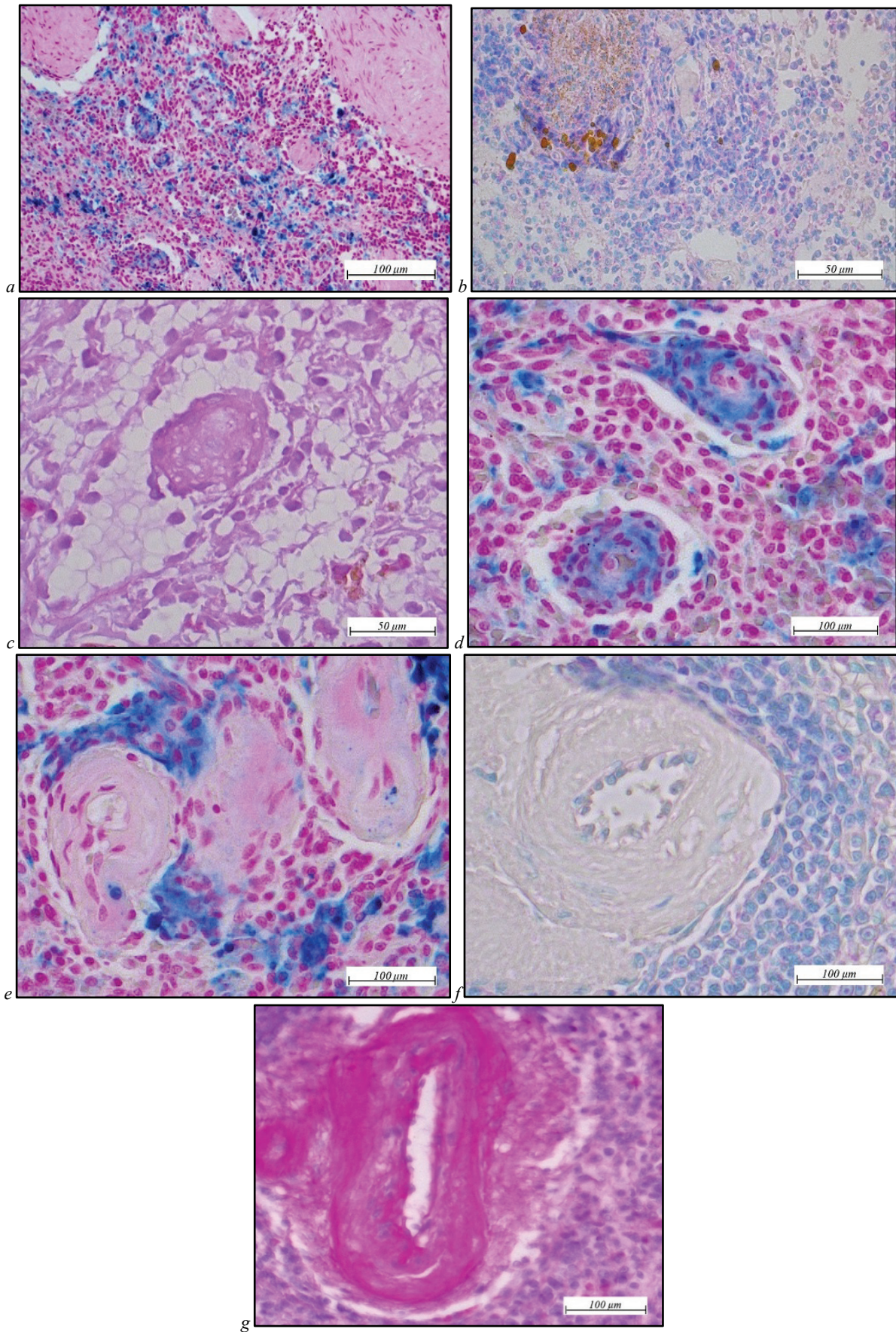


Fig. 3. The spleen of a dog poisoned with isoniazid (histological examination): *a* – spleen of a dog that died five hours after the onset of clinical symptoms; siderophages in the red pulp, Perls; *b* – siderophages in the lymph node, bracket; *c* – coagulated protein with exfoliated endothelium in the lumen of the venule, McManus; *d* – the lumen of the arterioles is closed and their walls are impregnated with hemosiderin, Perls; *e* – the structure of the walls of the arterioles is retouched; the nuclei of the fibers are lysed, Perls; *f* – arteries; the content of RNA in the cytoplasm and DNA in the nuclei of smooth muscle fibers is not detected, bracket; *g* – fuchsinophilic structures of the arterial wall, McManus

The formation of large quantities of hemosiderin prevented macrophages from destroying it. This is expressed by a significant increase in the number of hemosiderophages and the content of free hemosiderin in the white and red pulp (Fig. 2h). The number of hemosiderophages and the content of free hemosiderin in the structures of lymph nodes and red pulp increased significantly in the spleen of dogs during a long clinical course of poisoning (more than four hours).

The blood supply to the red pulp of the spleen was much decreased during the long clinical course of poisoning. The devastated lumens of the venous sinuses and loops of the reticular structures were observed (Fig. 3b). The reticular tissue permeated with venous sinuses was exposed. The lumens of the venous sinuses contained almost no blood elements. Instead, the peeled endotheliocytes visualized in the plexus of coagulated fuchsinophilic protein (Fig. 3c).

At the same time, narrowing of the arterioles' lumen and dystrophic changes in the elastic membrane and smooth muscle fibers were observed. The arterioles' elastic membrane was loosened and thickened, impregnated with an amorphous mass. The lumen of most brush arterioles was sharply narrowed. On preparations with Perls staining, the walls of some arterioles acquired a bluish colour, which indicated their impregnation with hemosiderin (Fig. 3d). Reduction of blood flow in arterioles and small arteries progressed. The endothelium of small arteries was swollen, the inner elastic membrane was thickened and the layer of smooth muscle fibers was retouched with their nuclei lysed. These phenomena indicated the progression of necrobiotic processes in the arterioles' walls (Fig. 3e).

The lumen was narrowed in the pulpal arteries of muscular type. Disorganization, plasma impregnation, and development of fibrinoid swelling of their walls were noted. Swollen endothelial cells protruded into the lumen of blood vessels. The inner elastic membrane of the intima was thickened. On preparations with Brachet staining, the content of RNA in the cytoplasm and DNA in the nuclei of smooth muscle fibers was not determined, apparently due to the progression of necrobiotic changes (Fig. 3f). On preparations with McManus staining, all structural elements of the arteries' walls were thickened and impregnated with glycoproteins (Fig. 3g).

Analyzing the morphohistochemical changes in the dogs' spleen, it should be noted that a sharp violation of hemodynamics and physicochemical properties of blood expressed itself functionally in the development of a hypoxic state. A sharp change in blood rheology was indicated by disorganization of vessel walls and connective tissue skeleton of the organ, dilatation of veins, their overflow with hemolyzed blood, plasma impregnation with the development of fibrinoid swelling, and necrosis of the arterioles and arterial walls. Increased intravascular hemolysis of erythrocytes contributed to a sharp decrease in metabolic processes and tissue oxygenation, an increase in the number of hemosiderophages, the content of free hemosiderin both in the red pulp and lymph nodules of the white pulp. Disorders in the cells' trophism and metabolism led to the progression of necrobiotic processes in lymphoid elements and connective tissue structures.

Lymph nodes, namely, parotid, superficial cervical, hepatic and splenic ones, were macroscopically round or oval, of greyish-brown or greyish-cherry colour. The connective tissue capsule was tense, smooth, and moist. Its section surface was moist and of brown or dark cherry colour.

The histopathological changes in the lymph nodes of dogs that died at various periods were slightly different. Obviously, they depended on the physiological condition of each animal and the received drug dose. A sharp violation of hemodynamics was a common feature in all cases. It was expressed by the dilatation of blood vessels, sinuses, and violation of the physicochemical properties of blood. In some animals, the vessels and sinuses were filled with blood. Blood elements diffused beyond the vessels. Hemosiderin, i.e., fine-grained golden-brown patches, visualized both perivascularly and in the vessel lumen (Fig. 4b). In other animals (in case of the long course of clinical signs), the content of blood in the lumen of sharply dilated vessels was absent (Fig. 4c).

The lymph nodules of the cortex preserved their structure and were densely populated with lymphoid cells (Fig. 4d). However, most of the lymphoid elements were in a state of karyorrhexis and lysis (Fig. 4e).

The lumen of the sinuses and venules was sharply expanded in the lymph nodes' medullary area. The venules did not contain blood elements. Endothelial cells were mostly desquamated and the basement

membrane was homogenized (Fig. 4f). The coastal endothelial cells of the cerebral sinuses acquired rounded shapes, lost their synthetic connections, and the cytoplasm contained a golden-brown pigment. Transforming into macrophages, endothelial cells changed shape and size and were freely located in the lumen of sinuses (Fig. 4g).

Intravascular hemolysis of erythrocytes activated the transformation of the lymph nodes' endothelial and reticular cells into siderophages. The histochemical reaction according to Perls showed that the cytoplasm of hypertrophied macrophages acquired the Prussian blue colour, indicating the presence of hemosiderin, an iron-containing pigment, in the cytoplasm of macrophages. Hemosiderin in its free state appears due to the hemolysis of erythrocytes. The growth of hemosiderin content in the lymph nodes stimulated the transformation of cerebral cords' reticular and endothelial cells into macrophages. Significantly more siderophages were found in the central sinuses of the dogs that died 5–6 hours after the onset of poisoning symptoms (Fig. 5a). The detected changes indicated disintegration of the sinuses' reticular network and disruption of the venules' basement membrane.

Obviously, the longer the course of toxicosis, the more pronounced the hemolysis of erythrocytes and consequently the higher content of the released hemosiderin, which the siderophages did not have enough time to destroy fully. Free hemosiderin was detected in the intercellular substance. At the same time, siderophages were randomly arranged at different stages of their decay in the dilated central sinuses (Fig. 5b).

On preparations stained according to McManus, siderophages of different sizes acquired a brown colour. Among the lymphoid elements of the cerebral cords, much larger cells were distinguished. Their cytoplasm was filled with golden grains, but more often with diffuse lumps of brown pigment, which merged and completely filled the entire cytoplasm (Fig. 5c).

Narrowed cerebral cords of lymph nodes were filled with cells. Plasma cells with weakly pyroninophilic cytoplasm were seen among the lymphocytes on Brachet-stained preparations. The reticular fibers of the sharply dilated central sinuses were disrupted, which indicated the disintegration of the sinuses' reticular network and the venules' basement membrane (Fig. 5d). Swelling and homogenization of the arteriole walls and their permeation with PAS-positive compounds were noted in the vessels of the cerebral zone on preparations with McManus staining. This indicated plasmorrhagia, accumulation of protein masses, and the development of fibrinoid swelling of the blood vessels' walls (Fig. 5e). The disintegration of elastic and reticular fibers of trabeculae and arteriole walls progressed.

Discussion

Isoniazid (INH), a drug widely used for the prevention and treatment of tuberculosis, is associated with a 1–2% risk of severe and potentially fatal hepatotoxicity. There is evidence that hydrazine, the INH metabolite, plays an important role in the mechanism of this toxicity. Metabolism of INH leads to the formation of hydrazine in direct and indirect ways. In both cases, the amide bond hydrolysis requires INH amidase activity (Sarich et al., 1999; Perwitasari et al., 2015; He et al., 2020).

Schmid et al. (2017) found that clinical signs of isoniazid toxicosis were observed in 134 of 137 (98%) dogs and included seizures ($n = 104$), signs of CNS damage without seizures (94), gastrointestinal (41), cardiovascular (19), urogenital (4), and respiratory abnormalities (1). The mechanisms underlying the toxic effects of isoniazid (INH) are still unclear, but there is growing evidence that INH, or hydrazine, its major metabolite, may interfere with mitochondrial function (Hassan et al., 2015). Metabolites of INH or INH (for instance, hydrazine) can cause mitochondrial damage, which in its turn leads to oxidative stress in mitochondria and impairs energy homeostasis (Boelsterli & Lee, 2014).

LD₅₀ of INH for dogs is estimated at 50 mg/kg, which is similar to that for humans. It is worth noting that rodents are among the species most resistant to INH. Therefore, they are not good animal models for extrapolating toxic doses. Recurrent clonic-tonic seizures accompanied by a stupor with poor response to the stimulus were more consistent clinical signs (Villar et al., 1995).

According to the studies, ALT and AST elevated in the model group and pathological examination of the liver showed damage to the liver tissue. The apoptotic index was higher than that of the control group ($7.13 \pm 1.55\%$ vs. $0.75 \pm 0.71\%$, $Z = -3.411$, $P < 0.01$).

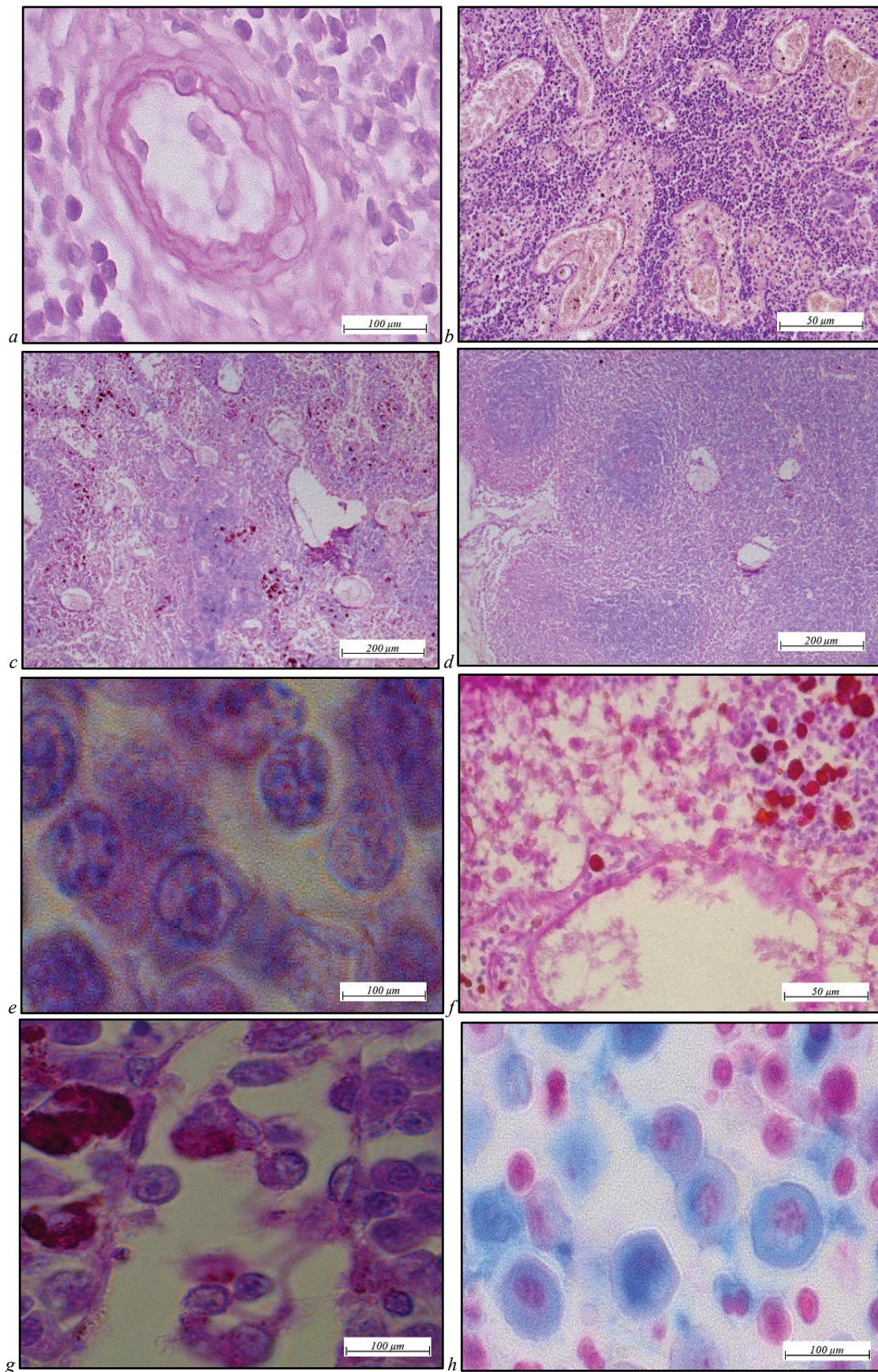


Fig. 4. The lymph node of a dog poisoned with isoniazid (histological examination): *a* – central artery of the lymph node; the basement membrane is swollen, fuchsinophilic, and the endothelium is desquamated, McManus; *b* – dilatation of blood vessels, blood overflow, and blood diffusion outside the vessels; *c* – brain area; there is no blood content in the dilated vessels; there are brown granular accumulations in the central sinuses; *d* – cortical area; the capsule is fibrous; lymph nodes are densely populated with lymphocytes; *e* – lymphoid elements in the state of karyorexis and lysis; *f* – the venule is expanded and contains blood elements; the wall is homogenized in some places; *g* – hypertrophy and brown pigment in the cytoplasm of sinus endothelial cells; *h* – central sinus of the lymph node; siderophages, Perls

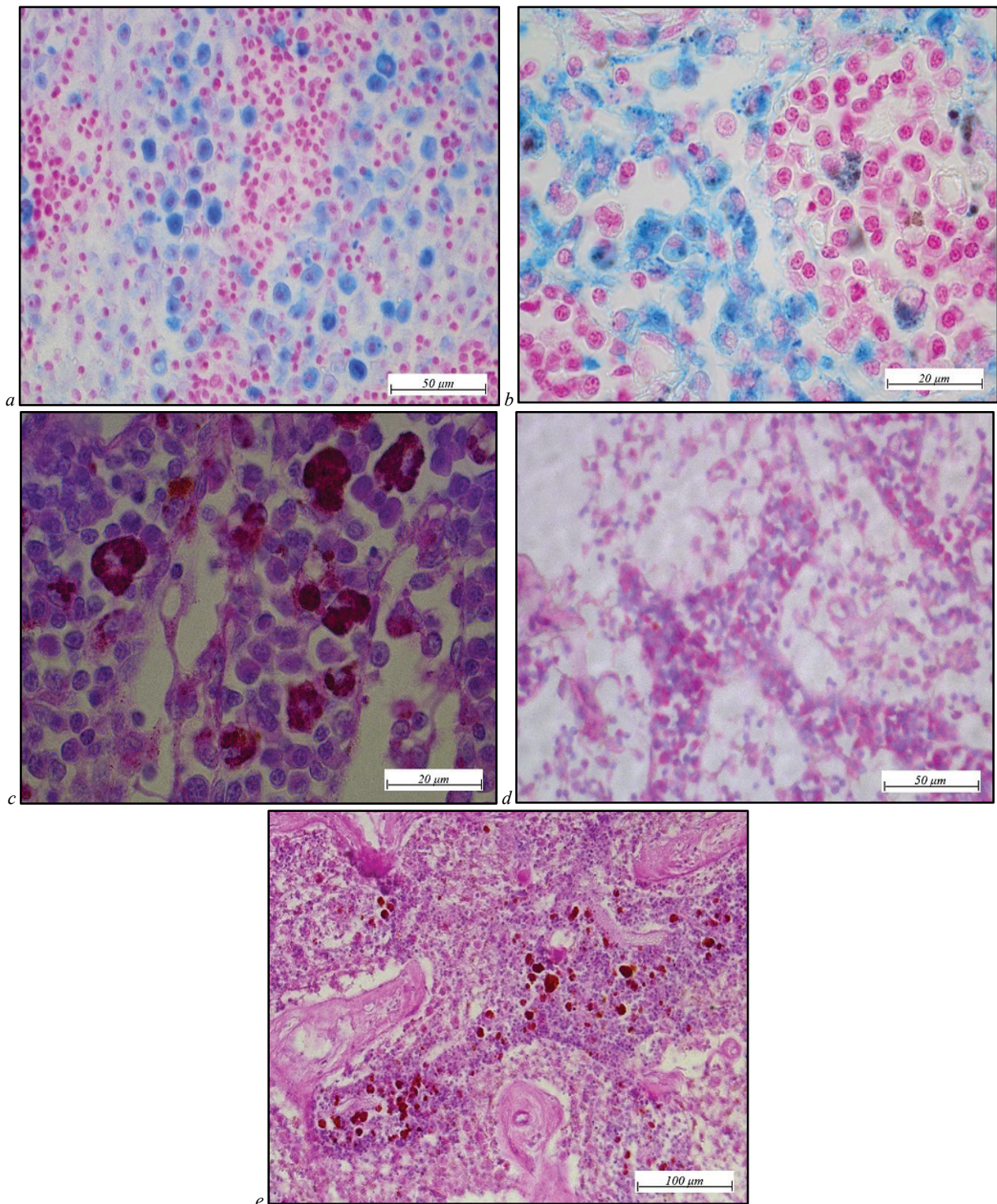


Fig. 5. The lymph node of a dog poisoned with isoniazid (histological examination): *a* – the central sinuses are filled with siderophages, Perls; *b* – central sinus of the lymph node, siderophages at different stages of decay; accumulation of hemosiderin in the intercellular substance, Perls; *c* – hemosiderophages in cerebral cords, McManus; *d* – the cerebral cords of the lymph node are narrowed; the disintegration of the reticular skeleton of the dilated sinuses, Brachet; *e* – trabeculae and arteriole walls are loosened and impregnated with PAS-positive compounds, McManus

The value of ERS protein expression in the model group was significantly higher than in the control group (GRP 78: 1.16 ± 0.30 vs. 0.23 ± 0.05 , $t = -6.008$, $P < 0.01$; CHOP: 0.98 ± 0.23 vs. 0.20 ± 0.10 , $t = -6.378$, $P < 0.01$) (Peng et al., 2019).

The anti-tuberculosis drug isoniazid plays an important role in pathological states like acute intermittent porphyria, anemia, hepatotoxicity, hypercoagulable state (deep vein thrombosis, pulmonary embolism or ischemic stroke), pellagra (vitamin B₃ deficiency), peripheral neuropathy, and vitamin B₆ deficiency (Brewer et al., 2020).

Lee et al. (2013) investigated the toxic effects of isoniazid on mice. It has been found that a pharmacological or genetic disorder of mitochondrial complex I caused by isoniazid exacerbates mitochondrial dysfunction, thereby damaging the hepatocellular system. Hydrazine, a metabolite of isoniazid, is an inhibitor of mitochondrial complex II (Lee et al., 2019). Recent studies showed that the underlying dysfunction of complex I can lead to the massive liver and cell damage caused by non-toxic INH concentrations, imposed on these mitochondrial deficits (Boelsterli & Lee, 2014). Pharmacogenetic and pharmacokinetic studies revealed polymor-

phism in enzymes involved in INH metabolism and detoxification. Major metabolic enzymes include N-acetyltransferase 2, cytochrome P450 2E1 and glutathione S-transferase. Various phenotypes of these enzymes can affect the rate of INH metabolism, leading to the formation of hepatotoxic metabolites (Erwin et al., 2019).

The study of isoniazid metabolites showed that patients with a fast acetylator phenotype hydrolyzed significantly more isoniazid to isonicotinic acid and the free hydrazine moiety than slow acetylators. The hydrazine moiety isolated from isoniazid is predominantly acetylhydrazine. Animal studies show this metabolite converts to a potent acylating agent, causing liver necrosis (Mitchell et al., 1976). For some animals, including dogs, drugs of this group are fatal even in small doses (Chuvina et al., 2018). The toxic effect of isoniazid depends on its dose. Toxic doses are estimated at 35–40 mg/kg, while lethal – at 150 mg/kg (Lahlou et al., 2019).

The study carried out by Pan et al. (2020) showed that isoniazid (INH) is mainly metabolized in the liver. A large amount of intracellular glutathione is consumed during the metabolism of this drug, which leads to lipid peroxidation and hepatocyte death (Pan et al., 2020). Liver histopathology revealed moderate cytoplasmic vacuolation, hepatocyte hypertrophy, ballooning, and necrosis (Souayed et al., 2015). It is known that excessive formation of hemosiderin leads to the development of general hemosiderosis. Earlier, in our publications on histochemical studies of changes in the kidneys and liver of dogs due to isoniazid poisoning, we found deposition of hemosiderin in the epithelium of the renal tubules and Kupffer cells in the liver.

Therefore, general hemosiderosis develops in the dog organism on the background of increased intravascular hemolysis of erythrocytes (Kotsiumbas & Vretsona, 2019). The toxic effect of isoniazid on the hematopoietic system of dogs is the reason for this process. In the spleen and lymph nodes, we revealed the disorganization of vessel walls and connective tissue skeleton of organs, dilatation of veins with their overflow with hemolyzed blood, development of mucoid swelling of arteriole walls with narrowing of their lumen and progression of dystrophic-necrobiotic changes in populations of lymphoid and stromal structural elements.

Conclusion

The vascular system of the lymph nodes provides drainage to all organs. Summarizing the results of the morphohistochemical study of the lymph nodes, it should be noted that isoniazid poisoning in dogs leads to a sharp expansion of the lumen of sinuses, venules and veins, collagen and disorganization of the reticular fibers, and transformation of reticular cells into siderophages. These changes are caused by hemolysis of the erythrocytes and indicate a sharp violation of hemodynamics and blood physicochemical properties. The result is a hypoxic state, metabolic disorders, acceleration of necrobiotic changes in the lymphoid elements of the cerebral cords, cortical and paracortical areas.

Reticular skeleton destruction, the transformation of reticular cells into hemosiderophages and the increase in their number in the red and white pulp of the spleen, central sinuses, and the pulp of the lymph nodes are caused by the excessive hemosiderin synthesis due to intravascular hemolysis of erythrocytes.

The morphological study of the peripheral organs of the immune system suggests that dogs with isoniazid poisoning experience progressive hemodynamic disorders and changes in blood physicochemical properties, i.e. hemolysis of erythrocytes and thrombosis. This underlies trophic disorders, metabolic malfunctions, and the development of dystrophic necrobiotic changes in all structural elements of the spleen and lymph nodes.

References

Boelsterli, U. A., & Lee, K. K. (2014). Mechanisms of isoniazid-induced idiosyncratic liver injury: Emerging role of mitochondrial stress. *Journal of Gastroenterology and Hepatology*, 29(4), 678–687.

Brent, J., Vo, N., Kulig, K., & Rumack, B. H. (1990). Reversal of prolonged isoniazid-induced coma by pyridoxine. *Archives of Internal Medicine*, 150(8), 1751–1753.

Brewer, C. T., Kodali, K., Wu, J., Shaw, T. I., Peng, J., & Chen, T. (2020). Toxicoprofiling of hPXR transgenic mice treated with rifampicin and isoniazid. *Cells*, 9(7), 1654.

Chin, L., Sievers, M. L., Herrier, R. N., & Picchioni, A. L. (1981). Potentiation of pyridoxine by depressants and anticonvulsants in the treatment of acute isoniazid intoxication in dogs. *Toxicology and Applied Pharmacology*, 58(3), 504–509.

Chin, L., Sievers, M. L., Laird, H. E., Herrier, R. N., & Picchioni, A. L. (1978). Evaluation of diazepam and pyridoxine as antidotes to isoniazid intoxication in rats and dogs. *Toxicology and Applied Pharmacology*, 45(3), 713–722.

Chuvina, N. A., Kachkina, M. A., & Strelova, O. Y. (2018). The chemical toxicological determination of isoniazid and metoclopramide in the objects used for animals poisoning and in biological fluids. *Sudebno-Meditsinskaya Ekspertisa*, 61(6), 33–38.

Erwin, E. R., Addison, A. P., John, S. F., Olaleye, O. A., & Rosell, R. C. (2019). Pharmacokinetics of isoniazid: The good, the bad, and the alternatives. *Tuberculosis*, 116S, S66–S70.

Hassan, H. M., Guo, H.-L., Yousef, B. A., Luyong, Z., & Zhenzhou, J. (2015). Hepatotoxicity mechanisms of isoniazid: A mini-review. *Journal of Applied Toxicology*, 35(12), 1427–1432.

He, X., Song, Y., Wang, L., & Xu, J. (2020). Protective effect of pyrrolidine dithiocarbamate on isoniazid/rifampicin induced liver injury in rats. *Molecular Medicine Reports*, 21(1), 463–469.

Kotsiumbas, H. I., & Vretsona, N. P. (2019). Histohichni ta histokhimichni zminy v nyrkakh sobak za otruiennia izoniazidom [Histological and histochemical changes in the kidneys of dogs due to isoniazid poisoning]. *Naukovo-Tekhnichnyj Biuletyn DNDKI Vetpreparativ ta Kormovykh Dobavok i Instytutu Biologii Tvaryn*, 20(2), 238–246 (in Ukrainian).

Kucenko, S. A. (2004). *Osnovy toksikologii* [Fundamentals of toxicology]. Foliant, Moscow (in Russian).

Kucenko, S. A., Butomo, N. V., & Grebenjuk, A. N. (2004). *Voennaja toksikologija, radiobiologija i medicinskaja zashhita* [Military toxicology, radiobiology and medical protection]. Foliant, Moscow (in Russian).

Lahlou, A., Benlammkadem, S., Berdai, M. A., & Harandou, M. (2019). Seizures following intoxication with a common antituberculosis drug. *Case Reports in Pediatrics*, 2019, 8972574.

Lee, K. K., Fujimoto, K., Zhang, C., Schwall, C. T., Alder, N. N., Pinkert, C. A., Krueger, W., Rasmussen, T., & Boelsterli, U. A. (2013). Isoniazid-induced cell death is precipitated by underlying mitochondrial complex I dysfunction in mouse hepatocytes. *Free Radical Biology and Medicine*, 65, 584–594.

Lee, L. N., Huang, C. T., Hsu, C. L., Chang, H. C., Jan, I. S., Liu, J. L., Sheu, J. C., Wang, J. T., Liu, W. L., Wu, H. S., Chang, C. N., & Wang, J. Y. (2019). Mitochondrial DNA variants in patients with liver injury due to anti-tuberculosis drugs. *Journal of Clinical Medicine*, 8(8), 1207.

Lheureux, P., Penaloza, A., & Gris, M. (2005). Pyridoxine in clinical toxicology: A review. *European Journal of Emergency Medicine*, 12(2), 78–85.

Mitchell, J. R., Zimmerman, H. J., Ishak, K. G., Thorgeirsson, U. P., Timbrell, J. A., Snodgrass, W. R., & Nelson, S. D. (1976). Isoniazid liver injury: Clinical spectrum, pathology, and probable pathogenesis. *Annals of Internal Medicine*, 84(2), 181–192.

Pan, Y., Tang, P., Cao, J., Song, Q., Zhu, L., Ma, S., & Zhang, J. (2020). Lipid peroxidation aggravates anti-tuberculosis drug-induced liver injury: Evidence of ferroptosis induction. *Biochemical and Biophysical Research Communications*, 533(4), 1512–1518.

Peng, X. Y., Luo, X. H., Yang, Q., Cheng, M. L., Han, B., & Xie, R. J. (2019). Inter-ventional effect of bicyclol on isoniazid-induced liver injury in rats and the expression of glucose-regulated protein 78, and growth arrest and DNA-damage-inducible gene 153. *Zhonghua Gan Zang Bing Za Zhi*, 27(2), 133–139.

Pervitasari, D. A., Athobari, J., & Wilffert, B. (2015). Pharmacogenetics of isoniazid-induced hepatotoxicity. *Drug Metabolism Reviews*, 47(2), 222–228.

Sarich, T. C., Adams, S. P., Petricca, G., & Wright, J. M. (1999). Inhibition of isoniazid-induced hepatotoxicity in rabbits by pretreatment with an amidase inhibitor. *Journal of Pharmacology and Experimental Therapeutics*, 289(2), 695–702.

Schmid, D. R., Lee, J. A., Wismer, T. A., Diniz, P. P. V. P., & Murtaugh, R. J. (2017). Isoniazid toxicosis in dogs: 137 cases (2004–2014). *Journal of the American Veterinary Medical Association*, 251(6), 689–695.

Souayed, N., Chennoufi, M., Boughattas, F., Haouas, Z., Maaroufi, K., Miled, A., Ben-Attia, M., Aouam, K., Reinberg, A., & Boughattas, N. A. (2015). Circadian variation in murine hepatotoxicity to the antituberculosis agent “isoniazide”. *Chronobiology International*, 32(9), 1201–1210.

Villar, D., Knight, M. K., Holding, J., Barret, G. H., & Buck, W. B. (1995). Treatment of acute isoniazid overdose in dogs. *Veterinary and Human Toxicology*, 37(5), 473–477.